

Article

Variable Step Size Methods of the Hybrid Affine Projection Adaptive Filtering Algorithm under Symmetrical Non-Gaussian Noise

Xingli Zhou ^{1,2}, Guoliang Li ¹, Hongbin Zhang ¹ and Xin Cao ^{2,3,*}

¹ School of Information and Communication Engineering, University of Electronic Science and Technology of China, Chengdu 610056, China

² School of Information Engineering, Southwest University of Science and Technology, Mianyang 621010, China

³ School of Electronic Science and Engineering, University of Electronic Science and Technology of China, Chengdu 610056, China

* Correspondence: caoxin@swust.edu.cn

Abstract: The idea of variable step-size was introduced into the Hybrid Affine Projection Algorithm (H-APA) and we propose two variable step size algorithms based on H-APA, which are called the Variable Step-Size Hybrid Affine Projection Algorithm (VSS-H-APA) and the Modified Variable Step-Size Hybrid Affine Projection Algorithm (MVSS-H-APA). These are two variable-step algorithms aim to further improve the robust performance and convergence speed of H-APA under non-Gaussian noise. This allows for faster convergence while maintaining stability. The MVSS-H-APA goes further than VSS-H-APA to estimate the noise in order to achieve better convergence performance. The proposed algorithm performs better than the existing algorithms in system identification under symmetric non-Gaussian noise.

Keywords: adaptive filtering; affine projection (AP); variable step-size; system identification; robustness



Citation: Zhou, X.; Li, G.; Zhang, H.; Cao, X. Variable Step Size Methods of the Hybrid Affine Projection Adaptive Filtering Algorithm under Symmetrical Non-Gaussian Noise. *Symmetry* **2023**, *15*, 1158. <https://doi.org/10.3390/sym15061158>

Academic Editors: Kejun Li, Yongliang Liang, Zhijie Liu and Aviv Gibali

Received: 27 April 2023

Revised: 17 May 2023

Accepted: 25 May 2023

Published: 26 May 2023



Copyright: © 2023 by the authors. Licensee MDPI, Basel, Switzerland. This article is an open access article distributed under the terms and conditions of the Creative Commons Attribution (CC BY) license (<https://creativecommons.org/licenses/by/4.0/>).

1. Introduction

The adaptive filtering algorithm is widely used in system identification, echo cancellation, interference suppression and channel equalization because it has stronger signal processing capability and more adaptability than traditional filtering algorithms. The least mean square (LMS) and normalized LMS algorithms have received widespread attention owing to the ease of implementation. However, one of their shortcomings is that they obtain slower convergence behavior when facing correlated inputs. The excellent performance of the Affine Projection Algorithm (APA) [1] in dealing with colored input is attributed to update filter parameters by using a multidimensional combination of past input signals.

However, the practical application scenarios of these algorithms often involve non-Gaussian noise, including Laplace noise, binary noise, uniform noise [2], and other forms of noise. Outliers generated by these types of noise can significantly degrade algorithm performance or even prevent it from working properly [3]. Therefore, improving the robustness of adaptive filtering algorithms under non-Gaussian noise environments is a critical area of research. Around 2010, Shao et al. applied sign algorithm (SA) to the APA in order to further optimize its performance and proposed the Affine Projection Sign Algorithm (APSA) [4], which achieved remarkable results in system identification.

Recently, a new AP-type algorithm, named the Hybrid Affine Projection Algorithm (H-APA) [5], has been proposed, which combines the advantages of the Affine Projection Robust Mixed Norm Algorithm (APRMNA) [6] and APSA to achieve better performance under non-Gaussian noise. Of course, there are also many other methods applied to improve the robustness of adaptive filtering algorithms [7–13]. For satisfying the contradictory requirements between fast convergence speed and small steady-state misalignment, studies

have used various methods to further improve the convergence speed and accuracy of APSA, such as various types of variable step, combined step methods [14–21], etc.

In this paper, our objective is to further enhance the performance of H-APA by utilizing a variable step size approach similar to that used in APSA, and we also aim to make further estimations and calculations to enhance its performance. We begin by providing a review of H-APA and two variable step size methods of APSA. In system identification, we evaluate the efficacy of the proposed algorithms by conducting simulations in symmetrical non-Gaussian noise environments.

2. Related Algorithms

In this section, we provide a review of the H-APA and two variable step size methods of APSA.

2.1. Hybrid Affine Projection Algorithm (H-APA)

Let us consider a system identification model [22] in which the desired output signal is described by:

$$d(i) = \mathbf{w}_0^T \mathbf{x}(i) + v(i), \quad (1)$$

where $\mathbf{w}_0 \in \mathbb{R}^{K \times 1}$ denotes the parameter of the model to be discriminated, $\mathbf{x}(i) = [x(i), x(i-1), \dots, x(i-K+1)]^T \in \mathbb{R}^{K \times 1}$ denotes the input signal, $[\cdot]^T$ is the transpose symbol of the matrix, $v(i)$ consists of background noise and impulsive noise, K is the filter length, and i denotes the time.

The output error signal of the model is defined as $e(i) = d(i) - \mathbf{w}^T(i)\mathbf{X}(i)$, where the desired output data vector $\mathbf{d}(i) = [d(i), d(i-1), \dots, d(i-M+1)]^T$, the data matrix $\mathbf{X}(i) = [x(i), x(i-1), \dots, x(i-M+1)]^T$, $\mathbf{w}(i)$ at instant i , and M is the projection order.

According to the [5], the weight update formula of H-APA is

$$\mathbf{w}(i+1) = \mathbf{w}(i) + \frac{\mu \mathbf{X}(i) e_{mg}(i)}{\|\mathbf{X}(i) \text{sgn}(e(i))\|_2}, \quad (2)$$

where μ is the step size, $e_{mg}(i) = \zeta \text{sgn}(e(i)) + 2(1 - \zeta)e(i)$, $\text{sgn}(\cdot)$ is symbolic functions, and ζ is an adjustable parameter in the range of $[0 - 1]$.

To prevent the denominator of (2) from being zero, a very small positive constant $\delta (\delta = 0^+)$ is added as follows:

$$\mathbf{w}(i+1) = \mathbf{w}(i) + \frac{\mu \mathbf{X}(i) e_{mg}(i)}{\|\mathbf{X}(i) e_{mg}(i)\|_2 + \delta}. \quad (3)$$

2.2. Two Variable Step-Size Methods of APSA

2.2.1. Variable Step-Size Affine Projection Sign Algorithm (VSS-APSA)

The update equation for the weight vector of regular APSA, as stated in [4], is recursive and can be expressed as follows:

$$\mathbf{w}(i+1) = \mathbf{w}(i) + \frac{\mu \mathbf{X}(i) \text{sgn}(e(i))}{\|\mathbf{X}(i) \text{sgn}(e(i))\|_2}. \quad (4)$$

Next, $\tilde{\mathbf{w}}(i) \triangleq \mathbf{w}_0 - \mathbf{w}(i)$ is defined as the misaligned weight. Substituting it into (4) yields

$$\tilde{\mathbf{w}}(i+1) = \tilde{\mathbf{w}}(i) - \frac{\mu(i) \mathbf{X}(i) \text{sgn}(e(i))}{\|\mathbf{X}(i) \text{sgn}(e(i))\|_2}. \quad (5)$$

Following the method of [20], the two sides of (5) are squared while deriving the expected value.

$$E(\tilde{\mathbf{w}}^T(i+1)\tilde{\mathbf{w}}(i+1)) = E(\tilde{\mathbf{w}}^T(i)\tilde{\mathbf{w}}(i)) - 2\mu(i) \quad (6)$$

$$E\left(\frac{\|\mathbf{e}(i)\|_1 - \text{sgn}(\mathbf{e}^T(i))\mathbf{v}(i)}{\|\mathbf{X}(i)\text{sgn}(\mathbf{e}(i))\|_2}\right) + \mu^2(i) \\ \triangleq E(\tilde{\mathbf{w}}^T(i)\tilde{\mathbf{w}}(i)) - f(\mu(i)), \quad (7)$$

where $E(\cdot)$ is the expectation, $\mathbf{v}(i) = [v(i), v(i-1), \dots, v(i-M+1)]^T$.

So, the optimal step size μ^* for APSA is the value of $\mu(i)$ when $f(\mu(i))$ is maximum,

$$\mu^* = E\left(\frac{\|\mathbf{e}(i)\|_1 - \text{sgn}(\mathbf{e}^T(i))\mathbf{v}(i)}{\|\mathbf{X}(i)\text{sgn}(\mathbf{e}(i))\|_2}\right). \quad (8)$$

Due to $E(|\mathbf{X}^T(i)\tilde{\mathbf{w}}^T(i)|)$, we can approximate $E\left(\frac{\text{sgn}(\mathbf{e}^T(i))\mathbf{v}(i)}{\|\mathbf{X}(i)\text{sgn}(\mathbf{e}(i))\|_2}\right)$ to zero.

Finally, according to the time-averaging method, the updated formula for $\mu(i)$ is defined as

$$\mu(i+1) = \alpha\mu(i) + (1-\alpha)\min\left(\frac{\|\mathbf{e}(i)\|_1}{\|\mathbf{X}(i)\text{sgn}(\mathbf{e}(i))\|_2}, \mu(i)\right), \quad (9)$$

where $\alpha(0 < \alpha < 1)$ is a smoothing factor.

2.2.2. Modified Variable Step-Size Affine Projection Sign Algorithm (MVSS-APSA)

The VSS-APSA approximates $E\left(\frac{\text{sgn}(\mathbf{e}^T(i))\mathbf{v}(i)}{\|\mathbf{X}(i)\text{sgn}(\mathbf{e}(i))\|_2}\right)$ in μ^* of the optimal step as zero. However, in the [18], it is computed as

$$E\left(\frac{\text{sgn}(\mathbf{e}^T(i))\mathbf{v}(i)}{\|\mathbf{X}(i)\text{sgn}(\mathbf{e}(i))\|_2}\right) \approx E\left(\frac{\|\mathbf{v}(i)\|_1}{\|\mathbf{X}(i)\text{sgn}(\mathbf{e}(i))\|_2}\right) \\ \approx E\left(\frac{KE|\mathbf{v}(i)|}{\|\mathbf{X}(i)\text{sgn}(\mathbf{e}(i))\|_2}\right) > 0. \quad (10)$$

Therefore, for MVSS-APSA, (8) is modified to

$$\mu(i+1) = \alpha\mu(i) + (1-\alpha)\min\left(\frac{\|\mathbf{e}(i)\|_1 - K\beta(i+1)}{\|\mathbf{X}(i)\text{sgn}(\mathbf{e}(i))\|_2}, \mu(i)\right), \quad (11)$$

where $E(|\mathbf{v}(i)|)$ is estimated as $\beta(i+1) = \lambda\beta(i) + (1-\lambda)|e(i)|$ ($0 \ll \lambda < 1$), $\beta(0) = 0$.

3. The Proposed Algorithms

From the previous section, we know that since the variable step-size method can significantly improve the convergence speed as well as the accuracy of the original algorithms, we apply the two variable step-size methods mentioned in the previous section to H-APA and propose the Variable Step-Size Hybrid Affine Algorithm (VSS-H-APA) and Modified Variable Step-Size Hybrid Affine Algorithm (MVSS-H-APA) in this section.

3.1. Variable Step-Size Hybrid Affine Algorithm (VSS-H-APA)

Similarly, we define $\tilde{\mathbf{w}}(i) \triangleq \mathbf{w}_o - \mathbf{w}(i)$ and import it into (2) to obtain

$$\tilde{\mathbf{w}}(i+1) = \tilde{\mathbf{w}}(i) - \mu(i)\frac{\mathbf{X}(i)\mathbf{e}_{mg}(i)}{\|\mathbf{X}(i)\text{sgn}(\mathbf{e}(i))\|_2}. \quad (12)$$

Let $\mathbf{h}(i) \triangleq E(\|\tilde{\mathbf{w}}(i)\|_2^2)$, also taking the expectation for both sides of the square of (11), we obtain

$$\mathbf{h}(i+1) = \mathbf{h}(i) - 2\mu(i)E\left(\frac{(\mathbf{X}(i)\mathbf{e}_{mg}(i))^T\tilde{\mathbf{w}}(i)}{\|\mathbf{X}(i)\text{sgn}(\mathbf{e}(i))\|_2}\right) + \mu^2(i), \quad (13)$$

we further define

$$\mathbf{h}(i+1) \triangleq \mathbf{h}(i) - f(\mu(i)), \quad (14)$$

where $f(\mu_i) = \mu^2(i) - 2\mu_i E\left(\frac{(\mathbf{X}(i)\mathbf{e}_{mg}(i))^T \tilde{\mathbf{w}}(i)}{\|\mathbf{X}(i)\text{sgn}(\mathbf{e}(i))\|_2}\right)$.

From (13), it can be seen that $f(\mu(i))$ can obtain a maximum value when $\mu(i) = \mu^*$, and $\mathbf{h}(i+1)$ has a minimum value, at this point

$$\begin{aligned} \mu^* &= E\left(\frac{(\mathbf{X}(i)\mathbf{e}_{mg}(i))^T \tilde{\mathbf{w}}(i)}{\|\mathbf{X}(i)\text{sgn}(\mathbf{e}(i))\|_2}\right) \\ &= E\left(\frac{\mathbf{e}_{mg}^T(i)\mathbf{X}^T(i)\tilde{\mathbf{w}}(i)}{\|\mathbf{X}(i)\text{sgn}(\mathbf{e}(i))\|_2}\right), \end{aligned} \quad (15)$$

substituting $\mathbf{e}_{mg}(i) = \zeta \text{sgn}(\mathbf{e}(i)) + 2(1 - \zeta)\mathbf{e}(i)$ into (14) yields

$$\mu^* = E\left(\frac{\zeta \|\mathbf{e}(i)\|_1 + 2(1 - \zeta) \|\mathbf{e}(i)\|_2 - \mathbf{e}_{mg}^T(i)\mathbf{v}(i)}{\|\mathbf{X}(i)\text{sgn}(\mathbf{e}(i))\|_2}\right), \quad (16)$$

although the value of $\mathbf{v}(i)$ is not known here, we can approximate $E\left(\frac{\mathbf{e}_{mg}^T(i)\mathbf{v}(i)}{\|\mathbf{X}(i)\text{sgn}(\mathbf{e}(i))\|_2}\right)$ as zero since the filter is in a transient state when $E(|\mathbf{X}^T(i)\tilde{\mathbf{w}}(i)|) > E(|\mathbf{v}(i)|)$ [20].

So, (15) can be rewritten

$$\mu^* = E\left(\frac{\mathbf{e}_{ng}(i)}{\|\mathbf{X}(i)\text{sgn}(\mathbf{e}(i))\|_2}\right), \quad (17)$$

where $\mathbf{e}_{ng}(i) = \zeta \|\mathbf{e}(i)\|_1 + 2(1 - \zeta) \|\mathbf{e}(i)\|_2$.

Finally, we perform the $\mu(i)$ update by time averaging

$$\mu(i+1) = \alpha\mu(i) + (1 - \alpha)\min\left(\frac{\mathbf{e}_{ng}(i)}{\|\mathbf{X}(i)\text{sgn}(\mathbf{e}(i))\|_2}, \mu(i)\right), \quad (18)$$

where $\alpha(0 < \alpha < 1)$ is a smoothing factor.

3.2. Modified Variable Step-Size Hybrid Affine Algorithm (MVSS-H-APA)

To rephrase, in the VSS-H-APA section, the calculation of the step size $\mu(i)$ update approximates $E\left(\frac{\mathbf{e}_{mg}^T(i)\mathbf{v}(i)}{\|\mathbf{X}(i)\text{sgn}(\mathbf{e}(i))\|_2}\right)$ as zero, but in this section, we will improve the estimation of this term as the adaptive filter approaches its optimal solution. Importing $\mathbf{e}_{mg}(i) = \zeta \text{sgn}(\mathbf{e}(i)) + 2(1 - \zeta)\mathbf{e}(i)$ into it yields

$$\begin{aligned} E\left(\frac{\mathbf{e}_{mg}^T(i)\mathbf{v}(i)}{\|\mathbf{X}(i)\text{sgn}(\mathbf{e}(i))\|_2}\right) &= E\left(\frac{(\zeta \text{sgn}(\mathbf{e}^T(i)) + 2(1 - \zeta)\mathbf{e}^T(i))\mathbf{v}(i)}{\|\mathbf{X}(i)\text{sgn}(\mathbf{e}(i))\|_2}\right) \\ &= E\left(\frac{\zeta \text{sgn}(\mathbf{e}^T(i))\mathbf{v}(i) + 2(1 - \zeta)\mathbf{e}^T(i)\mathbf{v}(i)}{\|\mathbf{X}(i)\text{sgn}(\mathbf{e}(i))\|_2}\right) \\ &\approx E\left(\frac{\zeta \|\mathbf{v}(i)\|_1 + 2(1 - \zeta)\mathbf{e}^T(i)\mathbf{v}(i)}{\|\mathbf{X}(i)\text{sgn}(\mathbf{e}(i))\|_2}\right) \\ &\approx \frac{\zeta ME|\mathbf{v}(i)| + E(2(1 - \zeta)Me^T(i)\mathbf{v}(i))}{E(\|\mathbf{X}(i)\text{sgn}(\mathbf{e}(i))\|_2)} > 0, \end{aligned} \quad (19)$$

the reason for taking the approximation here is $E(\|\mathbf{X}^T(i)\tilde{\mathbf{w}}(i)\|_1) < E(\|\mathbf{v}(i)\|_1)$ in the steady-state [18].

Next, we make a further approximation to $E(2(1 - \zeta)Me^T(i)v(i))$. From the common mathematical inequalities, we know that

$$|v(1)|^2 + |v(2)|^2 + \dots + |v(i)|^2 \geq \frac{(|v(1)| + |v(2)| + \dots + |v(i)|)^2}{i} \quad (20)$$

i.e.,

$$\|v(i)\|_2^2 \geq \frac{\|v(i)\|_1^2}{M}, \quad (21)$$

so,

$$\begin{aligned} E(2(1 - \zeta)Me^T(i)v(i)) &= E(2(1 - \zeta)M(\tilde{w}^T(i)\mathbf{X}(i) + v^T(i))v(i)) \\ &\approx E(2(1 - \zeta)M\|v(i)\|_2^2) \\ &\approx E(2(1 - \zeta)\|v(i)\|_1^2) \\ &\approx 2(1 - \zeta)E|v(i)|, \end{aligned} \quad (22)$$

substituting this into (18), we obtain

$$\begin{aligned} E\left(\frac{e_{mg}^T(i)v(i)}{\|\mathbf{X}(i)\text{sgn}(e(i))\|_2}\right) &\approx \frac{\zeta ME|v(i)| + 2(1 - \zeta)E|v(i)|}{E(\|\mathbf{X}(i)\text{sgn}(e(i))\|_2)} \\ &= \frac{(\zeta M + 2(1 - \zeta))E|v(i)|}{E(\|\mathbf{X}(i)\text{sgn}(e(i))\|_2)} \\ &= \frac{(\zeta M + 2(1 - \zeta))\beta(i)}{E(\|\mathbf{X}(i)\text{sgn}(e(i))\|_2)}, \end{aligned} \quad (23)$$

where $E(|v(i)|)$ is estimated as $\beta(i + 1) = \lambda\beta(i) + (1 - \lambda)|e(i)|$ ($0 << \lambda < 1$), $\beta(0) = 0$.

Finally, the step size $\mu(i)$ update formula of MVSS-H-APA is written by time averaging method

$$\mu(i + 1) = \alpha\mu(i) + (1 - \alpha)\min\left(\frac{e_{ng}(i) - (\zeta M + 2(1 - \zeta))\beta(i)}{\|\mathbf{X}(i)\text{sgn}(e(i))\|_2}, \mu(i)\right). \quad (24)$$

4. Simulation Analysis

We conducted simulation tests of the proposed algorithm in an application environment of system identification. In all tests, we have set the values of M , K , and σ to be 10, 64, and 0.00001, respectively. In this system identification scenario, the vector w_o to be identified is normally distributed with a mean of 0 and a variance of 1. The input signals are generated by passing a normal process with standard deviation equal to one through a filter with a first-order transfer function represented by $B(z) = \frac{1}{1 - 0.7z^{-1}}$. This filter attenuates the high-frequency components of the input signal and produces an output signal that depends on both the current and past values of the input signal. The output signal we want to obtain is being affected by unwanted noise, but we have specified that the ratio of the signal power to the noise power should be 30 decibels, which can help us quantify the level of noise present in the signal. (The signal-to-noise ratio here refers to the signal-to-noise ratio of the Gaussian white noise added to the output noise.) Moreover, the noise added to the desired output signal is impulsive and follows the α -stable distribution. Because α -stable distribution is a non-Gaussian noise model with heavy-tailed distribution, it can well simulate the collective attenuation characteristics of real noise [23]. Specifically, the noise signal is denoted as $v(t)$, and it follows the α -stable distribution with parameters α , β , γ , and δ . Unless otherwise stated, we have fixed the parameters of the α -stable distribution to be $V_{\alpha\text{-stable}} = [\alpha, \gamma, \beta, \delta] = [1.8, 0.1, 0, 0]$, for all subsequent tests. The $V_{\alpha\text{-stable}}$ parameters we selected are all parameters that make the distribution symmetric, i.e., $\beta = 0$. The parameters being referred to have the same definition as the ones that were defined by Shao

and Nikias [3]. The parameters μ_0 and α of MVSS-APSA is set to 0.5 and 0.9 in this paper, for the reason that $\mu_0 = 2$ and $\alpha = 0.9$ of that has better performance known through [18]. Based on the findings in [5], we set the mixing factor ζ to 0 for the H-APA, as it has been shown to result in better performance at this value. The step sizes used by the relevant algorithms in all experiments are labeled in the legend, and these step sizes are specifically designed to ensure that they converge with the same steady-state accuracy. In other words, the step sizes have been carefully chosen to achieve a common level of accuracy and stability in the convergence of the algorithms. The tests' outcomes are reported using the normalized mean-squared deviation (NMSD) metric, which is computed as follows: $\text{NMSD}(t) = 20 \log_{10}(\|w_o - w(t)\|_2 / \|w_o\|_2)$. The tests were repeated 1000 times to obtain an average result.

In test 1, we used a step size of 0.1 for both algorithms in the proposed VSS-H-APA. We assessed its performance by testing different values of the parameter α across a range of values such as 0.1, 0.3, 0.5, 0.7, 0.9, in comparison with the APSA, MVSS-APSA, and H-APA. The results of this test are presented in Figure 1. The observations from Figure 1 are as follows: (1) when using the proposed VSS-H-APA, setting the factor α to a smaller value (i.e., $\alpha = 0.1$) results in higher accuracy and faster convergence compared to the APSA, MVSS-APSA, and H-APA. In general, the proposed algorithm outperforms these other algorithms; (2) when the factor α is set to 0.1, the proposed VSS-H-APA demonstrates excellent performance.

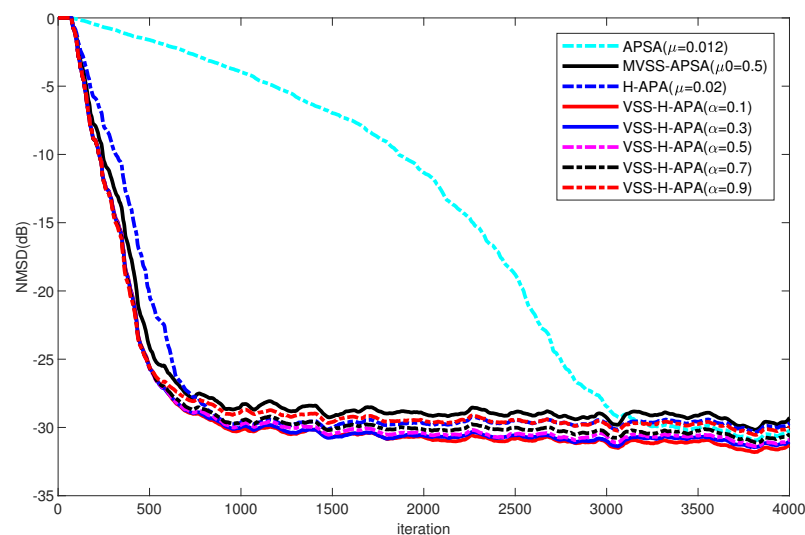


Figure 1. Simulated NMSD curves of APSA, MVSS-APSA H-APA and proposed VSS-H-APA.

In test 2, we evaluate the performance of the proposed MVSS-H-APA. In order to ensure a fair comparison between the various algorithms, we standardized the factor α of the VSS-H-APA to 0.1, as it demonstrated outstanding convergence speed and accuracy in test 1. Similar to test 1, we vary the factor α of the MVSS-H-APA across the range of values $\{0.1, 0.3, 0.5, 0.7, 0.9\}$. From Figure 2, we can make the following observations: (1) the proposed MVSS-H-APA outperforms the APSA, MVSS-APSA, and H-APA in terms of convergence speed and accuracy; (2) similar to the VSS-H-APA, using a smaller factor α (specifically, $\alpha = 0.1$) in the MVSS-H-APA results in excellent performance; (3) we discovered that when the factor α is set to 0.1, the MVSS-H-APA algorithm achieves fast convergence without sacrificing accuracy. Next, in Figure 3, we set the parameter α to 0.1 for both the VSS-H-APA and MVSS-H-APA and contrast their performance with the APSA, MVSS-APSA, and H-APA. Based on the results shown in Figure 3, it is evident that both the VSS-H-APA and MVSS-H-APA outperform APSA, MVSS-APSA, and H-APA under the specified parameters.

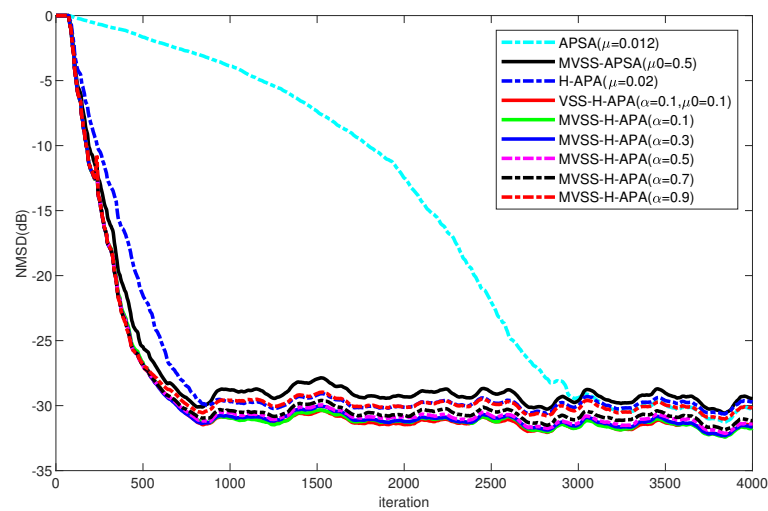


Figure 2. Simulated NMSD curves of APSA, MVSS-APSA H-APA and proposed VSS-H-APA and MVSS-H-APA.

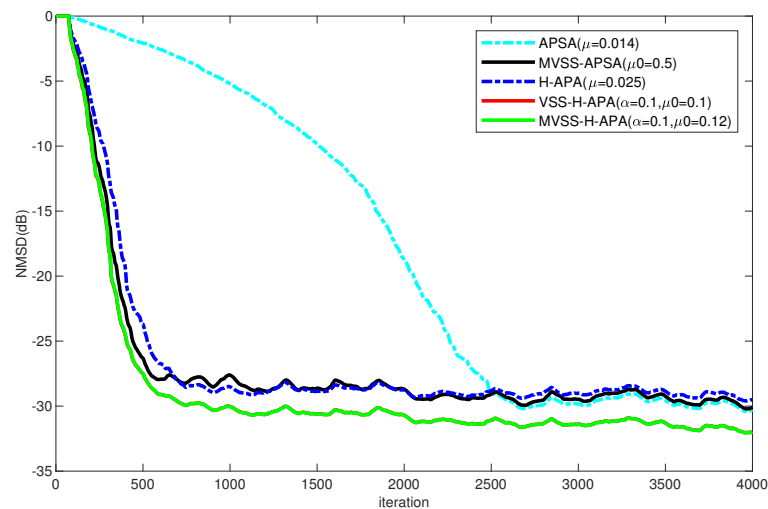


Figure 3. Simulated NMSD curves of APSA, MVSS-APSA, H-APA, VSS-H-APA and MVSS-H-APA.

In test 3, we updated the noise parameter vector $V_{\alpha-stable}$ from $[1.8, 0.1, 0, 0]$ to $[1.6, 0.1, 0, 0]$ based on the insights gained from analyzing the results presented in Figure 3 of test 2. To ensure a fair comparison between the performance of all algorithms, we adjust the step size such that the convergence accuracy remains approximately the same. Figure 4 shows the experimental results, from which we can conclude the following: (1) both the proposed VSS-H-APA and MVSS-H-APA exhibit the fastest convergence speed among all the tested algorithms; and (2) both the VSS-H-APA and MVSS-H-APA outperform APSA, MVSS-APSA, and H-APA in terms of convergence speed.

In test 4, we adjusted the signal-to-noise ratio to $[20 \text{ dB}, 10 \text{ dB}, 5 \text{ dB}]$ on the basis of Figure 4 to complete three simulations, as shown in Figures 5–7. We can observe that the proposed algorithms also have the best performance at different signal-to-noise ratios.

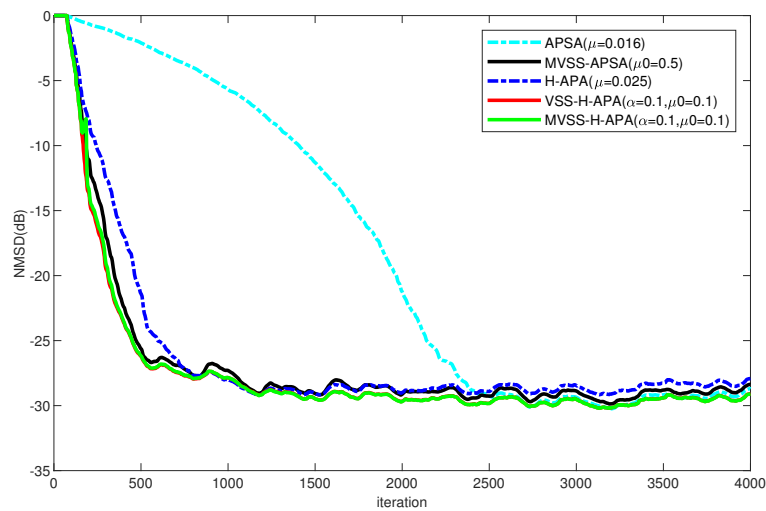


Figure 4. Simulated NMSD curves of APSA, MVSS-APSA, H-APA, VSS-H-APA and MVSS-H-APA with the $V_{\alpha-stable} = [1.6, 0.1, 0, 0]$.

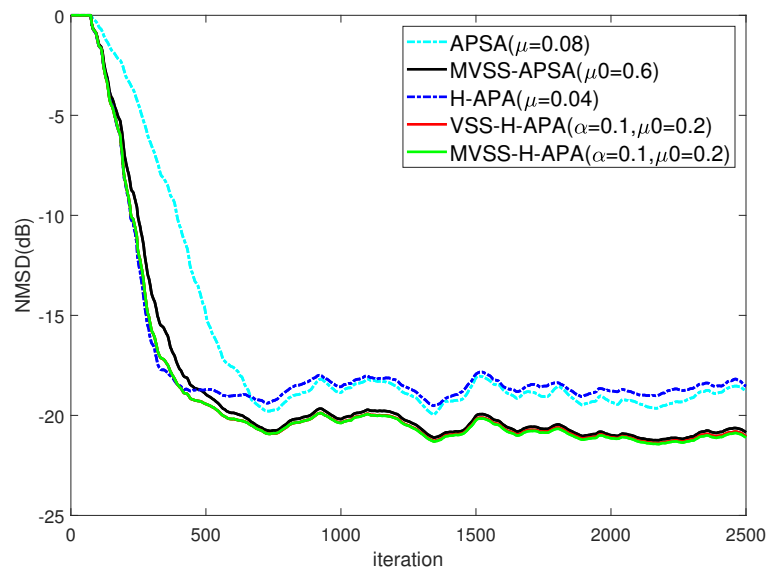


Figure 5. Simulated NMSD curves of APSA, MVSS-APSA, H-APA, VSS-H-APA and MVSS-H-APA with the SIR = 20 dB.

Overall, the results from all tests demonstrate that the proposed algorithms (i.e., VSS-H-APA and MVSS-H-APA) consistently outperform the APSA, MVSS-APSA, and H-APA algorithms in terms of convergence speed and accuracy. This suggests that the proposed algorithms are effective for solving impulsive noise.

(Remark: It is known from the selected experimental environment that MVSS-HAPA is slightly better than VSS-HAPA, but it cannot be excluded that VSS-HAPA performs better than MVSS-HAPA in other noisy environments.)

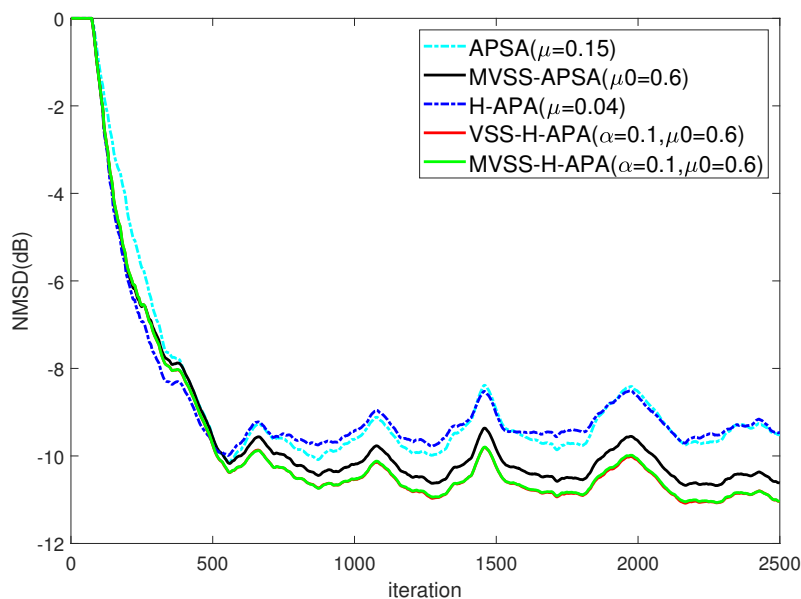


Figure 6. Simulated NMSD curves of APSA, MVSS-APSA, H-APA, VSS-H-APA and MVSS-H-APA with the SIR = 10 dB.

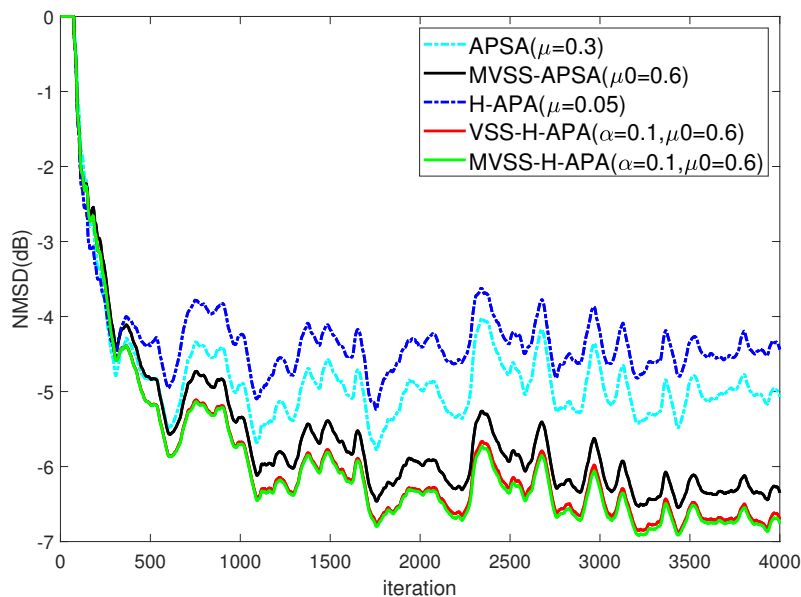


Figure 7. Simulated NMSD curves of APSA, MVSS-APSA, H-APA, VSS-H-APA and MVSS-H-APA with the SIR = 5 dB.

5. Conclusions

In this paper, we obtained VSS-H-APA and MVSS-H-APA by using a gradient descent method to iteratively update the step parameters and perform further estimation. When it comes to system identification simulation in the presence of impulse noise, the VSS-H-APA and MVSS-H-APA demonstrate superior performance compared to the existing APSA, MVSS-APSA, and H-APA.

Author Contributions: Methodology, software, writing—original draft, X.Z. and G.L.; writing—review and editing, project administration, funding acquisition, X.C. and H.Z. All authors have read and agreed to the published version of the manuscript.

Funding: This work was supported by Natural Science Foundation of Sichuan Province 2022NS-FSC0953.

Institutional Review Board Statement: Not applicable.

Informed Consent Statement: Not applicable.

Data Availability Statement: The data that support the findings of this study are available from the corresponding author upon reasonable request.

Conflicts of Interest: The authors declare no conflicts of interest.

References

1. Ozeki, K.; Umeda, T.; Members, R. An adaptive filtering algorithm using an orthogonal projection to an affine subspace and its properties. *Electron. Commun. Jpn.* **1984**, *67*, 126–132. [\[CrossRef\]](#)
2. Chen, B.; Xing, L.; Zhao, H.; Zheng, N. Generalized Correntropy for Robust Adaptive Filtering. *IEEE Trans. Signal Process.* **2016**, *64*, 3376–3387. [\[CrossRef\]](#)
3. Shao, M.; Nikias, C.L. Signal processing with fractional lower order moments: Stable processes and their applications. *Proc. IEEE* **1993**, *81*, 986–1010. [\[CrossRef\]](#)
4. Shao, T.; Zheng, Y.R.; Benesty, J. An affine projection sign algorithm robust against impulsive interferences. *IEEE Signal Process. Lett.* **2010**, *17*, 327–330. [\[CrossRef\]](#)
5. Zhou, X.; Li, G.; Wang, Z.; Wang, G.; Zhang, H. Robust hybrid affine projection filtering algorithm under α -stable environment. *Signal Process.* **2023**, *208*, 108981. [\[CrossRef\]](#)
6. Li, G.; Wang, G.; Dai, Y.; Sun, Q.; Yang, X.; Zhang, H. Affine projection mixed-norm algorithms for robust filtering. *Signal Process.* **2021**, *187*, 108153. [\[CrossRef\]](#)
7. Bhattacharjee, S.S.; Kumar, K.; George, N.V. Nearest Kronecker Product Decomposition Based Generalized Maximum Correntropy and Generalized Hyperbolic Secant Robust Adaptive Filters. *IEEE Signal Process. Lett.* **2020**, *27*, 1525–1529. [\[CrossRef\]](#)
8. Kumar, K.; Pandey, R.; Bhattacharjee, S.S.; George, N.V. Exponential Hyperbolic Cosine Robust Adaptive Filters for Audio Signal Processing. *IEEE Signal Process. Lett.* **2021**, *28*, 1410–1414. [\[CrossRef\]](#)
9. Kumar, K.; Karthik, M.L.N.S.; Bhattacharjee, S.S.; George, N.V. Affine Projection Champernowne Algorithm for Robust Adaptive Filtering. *IEEE Trans. Circuits Syst. II Express Briefs* **2022**, *69*, 1947–1951. [\[CrossRef\]](#)
10. Bhattacharjee, S.S.; Shaikh, M.A.; Kumar, K.; George, N.V. Robust Constrained Generalized Correntropy and Maximum Versoria Criterion Adaptive Filters. *IEEE Trans. Circuits Syst. II Express Briefs* **2021**, *68*, 3002–3006. [\[CrossRef\]](#)
11. Kumar, K.; Bhattacharjee, S.S.; George, N.V. Joint Logarithmic Hyperbolic Cosine Robust Sparse Adaptive Algorithms. *IEEE Trans. Circuits Syst. II Express Briefs* **2021**, *68*, 526–530. [\[CrossRef\]](#)
12. Kumar, K.; Karthik, M.L.N.S.; George, N.V. Generalized Modified Blake–Zisserman Robust Sparse Adaptive Filters. *IEEE Trans. Syst. Man Cybern. Syst.* **2023**, *53*, 647–652. [\[CrossRef\]](#)
13. Kumar, K.; Pandey, R.; Bora, S.S.; George, N.V. A Robust Family of Algorithms for Adaptive Filtering Based on the Arctangent Framework. *IEEE Trans. Circuits Syst. II Express Briefs* **2022**, *69*, 1967–1971. [\[CrossRef\]](#)
14. Ren, C.; Wang, Z.; Zhao, Z. A new variable step-size affine projection sign algorithm based on a posteriori estimation error analysis. *Circuits Syst. Signal Process.* **2017**, *36*, 1989–2011. [\[CrossRef\]](#)
15. Kim, J.; Chang, J.H.; Nam, S.W. Affine projection sign algorithm with l_1 minimization-based variable step-size. *Signal Process.* **2014**, *105*, 376–380. [\[CrossRef\]](#)
16. Shams Esfand Abadi, M.; Mesgarani, H.; Khademiyani, S.M. Robust variable step-size affine projection sign algorithm against impulsive noises. *Circuits Syst. Signal Process.* **2020**, *39*, 1471–1488. [\[CrossRef\]](#)
17. Yoo, J.; Shin, J.; Park, P. Variable Step-Size Affine Projection Sign Algorithm. *IEEE Trans. Circuits Syst. II Express Briefs* **2014**, *61*, 274–278. [\[CrossRef\]](#)
18. Zhang, S.; Zhang, J. Modified variable step-size affine projection sign algorithm. *Electron. Lett.* **2013**, *49*, 1264–1265. [\[CrossRef\]](#)
19. Cao, X.; Wang, C.; Li, W.; Cai, Q. An On-Chip Fractally Chipped FBAR Filter With Ba-Zn-Fe-Sc-O Thin Film in 5G-FR2 Millimeter-Wave Band. *IEEE Electron Device Lett.* **2023**, *44*, 682–685. [\[CrossRef\]](#)
20. Shin, J.; Yoo, J.; Park, P. Variable step-size affine projection sign algorithm. *Electron. Lett.* **2012**, *48*, 1. [\[CrossRef\]](#)
21. Huang, F.; Zhang, J.; Zhang, S. Combined-step-size affine projection sign algorithm for robust adaptive filtering in impulsive interference environments. *IEEE Trans. Circuits Syst. II Express Briefs* **2015**, *63*, 493–497. [\[CrossRef\]](#)
22. Ljung, T. A shift in paradigm for system identification. *Int. J. Control* **2020**, *93*, 173–180. [\[CrossRef\]](#)
23. Nolan, J.P. *Univariate Stable Distributions, Models for Heavy Tailed Data*; Springer: Berlin/Heidelberg, Germany, 2020.

Disclaimer/Publisher’s Note: The statements, opinions and data contained in all publications are solely those of the individual author(s) and contributor(s) and not of MDPI and/or the editor(s). MDPI and/or the editor(s) disclaim responsibility for any injury to people or property resulting from any ideas, methods, instructions or products referred to in the content.